13th World Conference on Earthquake Engineering
Vancouver, B.C., Canada
August 1-6, 2004
Paper No. 2614

LOCAL BUCKLING OF CFT-COLUMN UNDER SEISMIC LOAD

Motoo SAISHO[1], Masahiro KATO[2] and Shuyun GAO[3]

SUMMARY

Local buckling of concrete filled steel tube column (CFT column) is analyzed on the upper bound theorem of the limit analysis. The collapse mechanism of the analysis is assumed on the basis of CFT column test under monotonic and repeated load. The load deformation relations of many CFT columns designed under quite different conditions are calculated by the proposed analysis method. The plastic deformation capacity until the local buckling of CFT column which is closely related to the crack of steel tube is also obtained by it. From the calculated results it is shown that the local buckling of CFT column is significantly effected not only by the well known diameter to thickness ratio of steel tube but also by the axial force ratio, the aspect ratio and the strength ratio of filled-concrete to steel tube.

1. INTRODUCTION

The concrete filled steel tube column (CFT column) is useful as the earthquake resistant element because of its high strength and ductility. But in some cases under strong seismic load the CFT column fractures by the crack of steel tube[1)-3)]. The fracture of CFT column is brittle and works to collapse the whole CFT frame under strong ground motion[4)-6)].

The local buckling of CFT column under strong seismic load is not only related to degrade the restoring force of it but also to the steel tube crack of CFT column. Accordingly the effect of local buckling can not be neglected in the earthquake resistant design of CFT frame. In this study the analysis method of local buckling of CFT column is obtained on the upper bound theorem of the limit analysis. From the calculated results by the proposed method, the design factors and the design conditions of CFT column in the earthquake resistant design of CFT frame are investigated.

[1] Professor, Kumamoto Univ., Kumamoto, Japan. Email: saisho@gpo.kumamoto-u.ac.jp
[2] Professor, Aichi Sangyo Univ., Aichi, Japan.
[3] Graduate student, Kumamoto Univ., Kumamoto, Japan.

2. CFT COLUMN TEST

2.1 Specimens and loading conditions

Local buckling of CFT columns under axial load (N) and lateral load (H) have tested by the use of the cross-formed specimens with CFT column and H-section beam as shown in Fig.1. The CFT columns of specimen are explained in Table 2. In the table there are also the axial force ratio (N/N_u), the column length (L_c) and the compression strength of filled concrete (σ_c). The plastic deformation of CFT column $(\phi_{lb}/\phi_u)_T$, $(\phi_{lb}/\phi_u)_A$ until the local buckling of steel tube obtained by the test and the proposed analysis method explained later are also in the table. The material properties of steel tube are in Table.1.

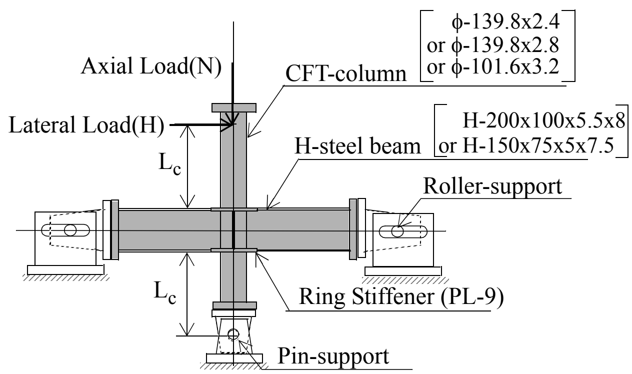

Fig.1 CFT Loading conditions of CFT column specimen

Table.1 Material properties of steel tube

Circular steel tube	σ_y	σ_u	ε_u
ϕ-101.6x3.2	378	455	23.8
ϕ-139.8x2.8	341	443	28.8
ϕ-139.8x2.4	463	549	22.6

Notations :
σ_y : yield stress (N/mm^2)
σ_u : tensile strength (N/mm^2),
ε_u : (%)

Table-2(A) Specimens and test results (ϕ139.8x2.4)

Specimen	Load	N/N_u	L_c	D/t	σ_c	r	$(\phi_{lb}/\phi_u)_T$	$(\phi_{lb}/\phi_u)_A$
SCTDI-S-60.10	D I	0.103	363	58.1	135	3.40	7.3	2.7
SCTDI-H-60.20	“ “	0.161	363	57.7	71	1.77	7.7	2.9
SCTDI-L-60.45	“ “	0.437	362	57.9	39	0.99	4.8	2.4
SCTDI-L-60.25	“ “	0.226	362	57.9	39	0.99	8.7	3.3
SCTDR-H-60.20	D R	0.200	363	58.1	71	1.79	8.2	2.5
SCTDR-L-60.20	“ “	0.200	362	57.9	39	0.99	6.0	3.6
SCTSM-H-60.30	S M	0.300	363	58.6	44	1.11	9.5	2.6
SCTSC-S-60.20	S C	0.198	363	57.4	135	3.35	6.6	1.6
SCTSC-S-60.10	“ “	0.100	363	57.4	118	2.92	9.7	3.1
SCTSC-H-60.20	“ “	0.161	362	57.7	71	1.77	8.2	2.9
SCTSC-L-60.45	“ “	0.450	362	57.9	39	0.99	4.2	2.4
SCTSC-L-60.20	“ “	0.200	362	57.9	39	0.99	4.6	3.6
LCTDI-S-60.20	D I	0.203	726	58.6	113	2.87	2.9	1.4
LCTDI-L-60.25	“ “	0.250	726	58.6	44	1.12	4.4	2.2

Table-2(B) Specimens and test results (ϕ139.8x2.8)

Specimen	Load	N/N_u	L_c	D/t	σ_c	r	$(\phi_{lb}/\phi_u)_T$	$(\phi_{lb}/\phi_u)_A$
SCTDI-S-50.25	D I	0.227	362	50.4	117	3.14	9.9	1.9
SCTDI-H-50.20	" "	0.191	362	50.4	57	1.54	12.4	3.8
SCTDI-L-50.45	" "	0.449	363	50.4	30	0.79	8.6	4.4
SCTDC-H-50.25	D C	0.250	363	50.4	71	1.90	11.5	2.7
SCTSM-L-50.15	S M	0.149	362	50.5	37	0.99	9.3	5.7
LCTDI-S-50.20	D I	0.200	724	50.5	113	3.04	5.4	2.5
LCTDI-L-50.25	" "	0.205	726	50.5	42	1.13	3.5	3.9

Table-2(C) Specimens and test results (ϕ101.6x3.2)

Specimen	Load	N/N_u	L_c	D/t	σ_c	r	$(\phi_{lb}/\phi_u)_T$	$(\phi_{lb}/\phi_u)_A$
SCTDI-S-30.25	D I	0.247	250	34.2	136	2.33	9.9	3.0
SCTDI-S-30.10	" "	0.108	249	34.2	128	2.20	8.4	7.1
SCTDI-H-30.20	" "	0.196	250	34.0	44	0.75	9.4	7.9
SCTDI-L-30.25	" "	0.264	249	34.0	18	0.30	17.1	10.9
SCTSI-S-30.25	S I	0.248	250	34.2	136	2.33	9.1	3.0
SCTSI-S-30.10	" "	0.108	249	34.2	128	2.20	13.7	7.1
SCTSI-L-30.25	" "	0.264	249	34.0	18	0.30	10.4	10.9
LCTDI-S-30.25	D I	0.254	502	34.2	131	2.25	7.7	2.5

Name of specimen:
S CT D I-S-60.20
1 2 3 4-5- 6 .7

1: Column length (S: L_c/D=2.5, L: L_c/D=5.0)
2: Concrete filled steel tube (CT)
3: Static loading (S), Dynamic loading (D)
4: Deformation wave
I: Incremental amplitude deformation,

C: Constant amplitude deformation,
R: Random wave
M: Monotonic loading
5: Compression strength of concrete (S, H, L)
6: Diameter to thickness ratio (D/t=60, 50, 30)
7: Axial force ratio(N/N_u, $N_u=\sigma_c A_c+\sigma_u A_s$)

Notations:
L_c : Column length (mm)
D/t : Diameter to thickness ratio
σ_c : Compression strength of concrete (N/mm^2)
r : Strength ratio of concrete to steel tube ($=\sigma_c A_c/\sigma_u A_s$)
$(\phi_{lb}/\phi_u)_T$: Plastic deformation of test until local buckling of steel tube
$(\phi_{lb}/\phi_u)_A$: Plastic deformation of calculation until local buckling of steel tube
ϕ_u : Upper bound of elastic deformation

2.2 Local buckling of CFT column specimen

In the CFT column test the axial strain (${}_A\varepsilon_i$, i: number of strain) and the circumferential strain (${}_T\varepsilon_i$) of steel tube in every 5mm distance from the column end were measured. By the use of the measured strains the local buckling of specimen is investigated.

Fig.2 shows the relation between the axial strain and the deformation of CFT column (ϕ_c). In the axial strains in the sections distant 15mm-60mm from the column end, only ${}_A\varepsilon_6$ and ${}_A\varepsilon_7$ change extremely the ratio of incremental strain to incremental deformation near the point B in the figure. This behavior expressed by the strain-deformation relation shows the local buckling of CFT column. The deformation of CFT column (ϕ_{lb}) when the steel tube buckled locally was obtained by this behavior and shown in Table.2(A)-Table.2(C).

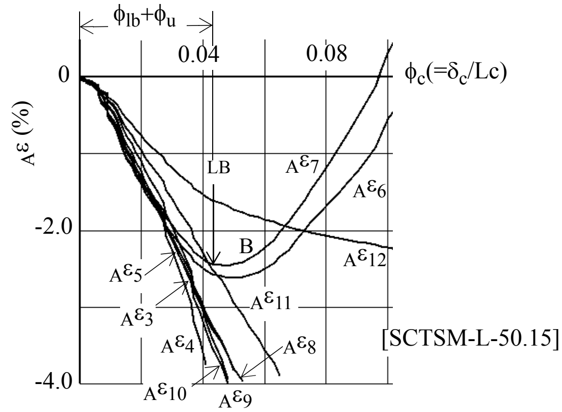

Fig.2 Relation between axial strain and CFT column deformation

2.3 Strain distribution of steel tube

Fig.3 shows the relations between the circumferential strain ($_T\varepsilon_i$) and the axial strain ($_A\varepsilon_i$) in the sections distant 15mm-60mm from the column end. In the figure the strains in the compression stress side and the tension stress side of the CFT column are explained. The compression side strains and the tension side strains appear only in the second quadrant and the fourth quadrant in the figure respectively. These results show that the circumferential strains in the compression side are quite different from the tension side strains of CFT column. The circumferential strains in the compression stress side are tension strain and the circumferential strains in the tension stress side are compression strain. The strain distribution obtained here is applied to assume the collapse mechanism of local buckling analysis.

The axial strain distribution in every loading step is shown in Fig.4. The strains in the figure are in the compression stress side strains. The axial strain are constant along the column axis (Z) in the small deformation of CFT column and after that the strain distribution along the column axis changes suddenly at some loading step. The change of the axial strain distribution means the steel tube buckled locally at this point.

The change of the axial strain distribution also shows the steel tube deformation by the local buckling. We can see that the local buckling deformation of specimen appeared in the range of the calculated local buckling length (L_b) as shown in Fig.4. The steel tube deformation by the local buckling obtained here was also used to assume the collapse mechanism of local buckling analysis.

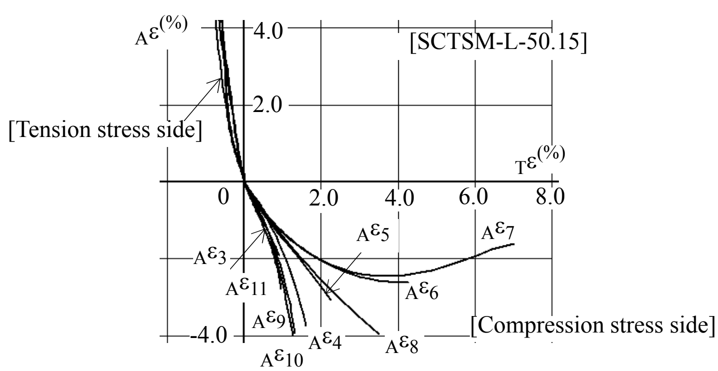

Fig.3 Relation between axial strain and circumferential strain

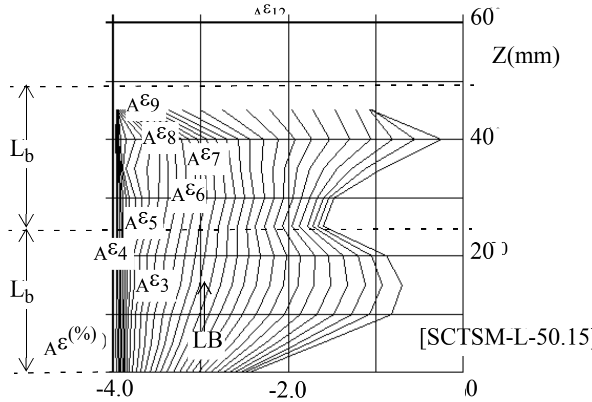

Fig.4 Distribution of axial strain in the compression stress side

3. LOCAL BUCKLING ANALYSIS CFT COLUMN

3.1 Collapse mechanism of local buckling

Local buckling of concrete filled steel tube column is analyzed on the upper bound theorem of the limit analysis. The collapse mechanism of the limit analysis, shown in Fig.5, is assumed as follows on the basis of CFT column test mentioned above.

a) Collapse mechanism of local buckling is expressed by the yield surfaces CPQ, CPR and the yield lines CQ, CP, CR as shown in Fig.5. In the surfaces the steel tube deforms in the circumferential direction but it does not deform in the axial direction. The deformation of steel tube is expressed by $\xi(z, \varphi)$ which is the parabolic function of φ as shown in Fig.6.

b) In the tension stress side of CFT column, there is the yield surface ABC in which only axial plastic strain is generated.

c) Except the yield surfaces CPQ, CPR, ABC and the yield lines CQ, CP,CR, the steel tube is assumed to be rigid. It is also assumed that there is not the slip between the filled concrete and steel tube.

d) The concrete strain surrounded by the yield surfaces CPQ, CPR is compression strain and the concrete strain surrounded by the yield surfaces ABC is tension strain.

e) The stress-strain relation of steel tube is assumed to be rigid-plastic relation. The stress-plastic strain relation of filled concrete is also approximated by the rigid-plastic relation which degrades linearly with plastic strain.

f) L_y, L_b, L_n are the length of plastic zone, the local buckling length and the distance of neutral axis from the center of section.

3.2 Load deformation relation of CFT column

By the use of the collapse mechanism mentioned above, the equation to express the load-deformation relation of locally buckled CFT column is derived on the basis of the upper bound theorem of the limit analysis. The equation of load-deformation relation is derived from the virtual work equation of the assumed collapse mechanism. Each component of the internal work and the external work in the virtual work equation are explained in the following equations.

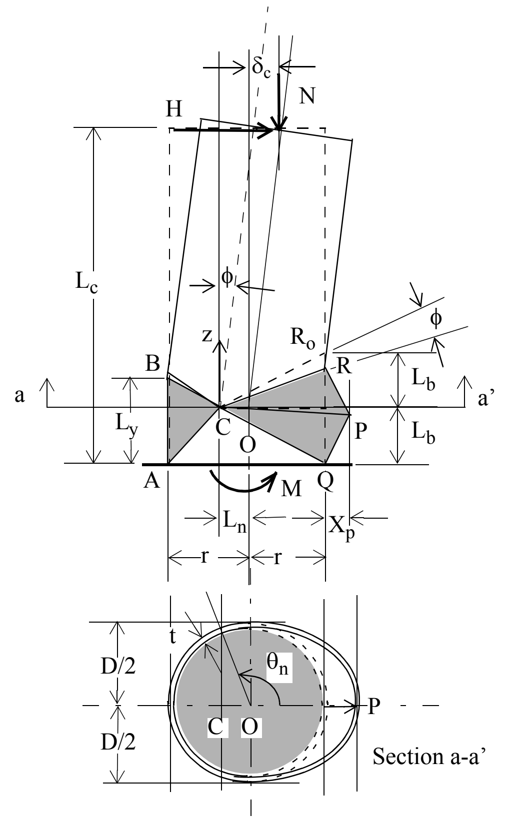

Fig.5 Collapse mechanism to express local buckling of steel tube

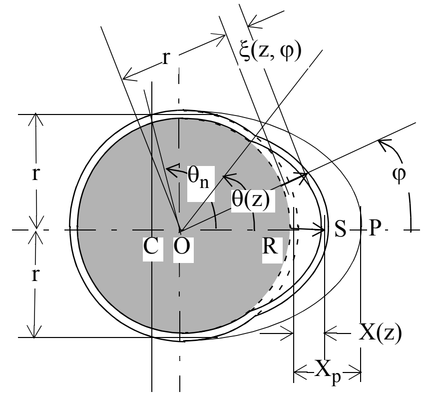

Fig.6 Local buckling deformation in the z-section

i) Internal work in the yield surface on the compression stress side (W_{IC})

In the yield surface CPQ, CPR (Fig.5), there are only circumferential stress (σ_t) (Assumption-a)) and the internal work in this yield surface is given by Eq.(1).

$$W_{IC} = \int(\sigma_t \Delta\varepsilon_t)dV \tag{1}$$

in which $\Delta\varepsilon_t$: the increment of circumferential strain, $\sigma_t = \sigma_u$ (Assumption-e)) and $\int dV$: the integration with the yield surface CPQ, CPR (Fig.5).

According to the Assumption-a), the local buckling deformation of steel tube can be expressed by $\xi(z,\varphi)$ (z: axial coordinate, φ: polar coordinate) in Eq.(2).

$$\xi(z, \varphi) = X(z)\left[1 - \left\{\frac{\varphi}{\theta(z)}\right\}^2\right] \tag{2}$$

In Eq.(2), $\theta(z)$ and $X(z)$ show the range that the steel tube deforms and the deformation at $\varphi=0$ as shown in Fig.6.

The circumferential strain of steel tube (ε_t), which is generated by the deformation $\xi(z,\varphi)$ in the range $-\theta(z)<\varphi<\theta(z)$, is given by Eq.(3).

$$\varepsilon_t = \frac{2}{3} \cdot \frac{X(z)}{r} \tag{3}$$

in which $r=(D-t)/2$, D: diameter of steel tube, t: thickness of steel tube.

$X(z)$-X_p relation can be obtained by the condition that RP, PQ (Fig.5) are straight because the steel tube does not deform in the axial direction (Assumption-a)). Except the yield surfaces and yield lines CFT column is assumed rigid (Assumption-c)). From this condition X_p-ϕ relation (ϕ: deformation angle of column (Fig.5)) is decided. By the use of $X(z)$-X_p relation and X_p-ϕ relation, $X(z)$ is expressed by the column deformation (ϕ) and ε_t in Eq.(3) is also expressed by the function of ϕ as shown in Eq.(4).

$$\varepsilon_t = \frac{2}{3}\frac{L_b}{r}\left(1-\frac{z}{L_b}\right)\left\{1-\left(1-\frac{L_n+r}{2L_b}\phi\right)^2\right\}^{1/2} \tag{4}$$

The incremental strain ($\Delta\varepsilon_t$) is derived from Eq.(4) and expressed by Eq.(5) by introducing Φ_c.

$$\Delta\varepsilon_t = \Phi_c\,\Delta\phi \tag{5}$$

Substituting $\sigma_t(=\sigma_u)$ and $\Delta\varepsilon_t$ into Eq.(1), W_{IC} becomes to be the function of $\Delta\phi$ as Eq(6).

$$W_{IC} = (\sigma_u)(\int\Phi_c dV)\Delta\phi \tag{6}$$

ii) Internal work in the yield lines (W_{IL})

The internal work (W_{IL}) in the yield lines CQ, CP, CR (Fig.5) is expressed by Eq.(7) in which m: the bending moment per length about the yield lines, $\Delta\Psi$: the incremental rotation about yield line.

$$W_{IL} = \int(m\cdot\Delta\psi)dL \tag{7}$$

The bending moment (m) is approximated by Eq.(8) neglecting the effects of the axial stress and the circumferential stress of steel tube on it.

$$m = \frac{1}{4}t^2\sigma_u \tag{8}$$

The rotation about yield line (Ψ) varies along the yield line because the deformation of steel tube ($\xi(z,\varphi)$) is expressed by the function of the polar coordinate (φ) as Eq.(2). But the change of rotation along the yield lines is small. From this reason the rotation (Ψ) is approximated by the rotation in the section of $\varphi=0$ as shown in Eq.(9).

$$\psi = \mathrm{acos}\left(1-\frac{L_n+r}{2L_b}\phi\right) \tag{9}$$

The values of m, Ψ in Eq.(8) and Eq.(9) are constant along the yield lines and the integration in Eq.(7) can be carried out simply as shown in Eq.(10).

$$W_{IL} = \left(\int_{CQ} dL + \int_{CR} dL + 2\int_{CP} dL\right)m\frac{1}{\sin\psi}\frac{L_n+r}{2L_b}\Delta\phi \tag{10}$$

In Eq.(10), $\int_{CQ} dL$, $\int_{CR} dL$, $\int_{CP} dL$ mean the integration along the yield lines CQ, CR, CP (Fig.5) respectively.

iii) Internal work in the yield surface on the tension stress side (W_{IT})

The work in the tension-side yield surface (W_{IT}) is given by the axial stress (σ_a) and the incremental axial strain ($\Delta\varepsilon_a$) as shown in Eq.(11).

$$W_{IT} = \int_T(\sigma_a\Delta\varepsilon_a)dV \tag{11}$$

In Eq.(11) $\sigma_a=\sigma_u$ from Assumption-b), Assumption-e) and $\int_T dV$ means the integration in the yield surface

(AB_oC).
When the CFT column deforms as shown in Fig.5, the steel tube section B_oC moves to BC as explained in Fig.7 and the axial strain ε_a is given by δ_a/L_x in which L_x, δ_a are the initial length (DE_o) and the extension (EE_o) of steel tube.

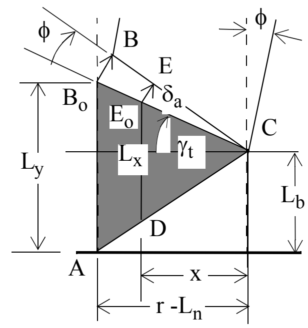

Fig.7 Yield surface and tension deformation in the tension stress side

The incremental axial strain $\Delta\varepsilon_a$ becomes to be the function of $\Delta\phi$ as shown in Eq.(12).

$$\Delta\varepsilon_a = \frac{r - L_n}{L_y}\frac{1}{\cos\gamma_t}\Delta\phi \tag{12}$$

in which γ_t is the angle to define the tension-side yield surface (Fig.7).
Substituting σ_a and $\Delta\varepsilon_a$, the internal work in the yield surface (W_{IT}) is expressed by the function of $\Delta\phi$ as Eq.(13).

$$W_{IT} = \left(\int_T dV\right)(\sigma_u)\frac{r - L_n}{L_y}\frac{1}{\cos\gamma_t}\Delta\phi \tag{13}$$

iv) Internal work in the filled concrete (W_{ICO})
According to the Assumptions-d) and Assumption-e), the internal work in the filled concrete (W_{ICO}) is decided by the concrete stress surrounded by the local buckling area of steel tube CQR_o (Fig.5).

$$W_{ICO} = \int_C (\sigma_{co}\Delta\varepsilon_{co})dV \tag{14}$$

In Eq.(14) σ_{co} and $\Delta\varepsilon_{co}$ are the compression strength and the incremental compression strain of filled concrete respectively. $\int_C dV$ means the integration in the filled concrete surrounded by the steel tube CQR_o. The filled concrete except that surrounded by the yield surface of steel tube is approximated to be rigid (Assumption-c)). From this reason the compression strain of concrete (ε_{co}) generated by the column deformation (ϕ) is constant and expressed by Eq.(15).

$$\varepsilon_{co} = \frac{L_n + r}{2L_b}\phi \tag{15}$$

The incremental compression strain of concrete ($\Delta\varepsilon_{co}$) is given by Eq.(16)

$$\Delta\varepsilon_{co} = \frac{L_n + r}{2L_b}\Delta\phi \tag{16}$$

The incremental compression strain of concrete ($\Delta\varepsilon_{co}$) expressed by Eq.(16) is substituted in Eq.(14), we get Eq.(17) as the internal work in the filled concrete (W_{ICO}) expressed by $\Delta\phi$.

$$W_{ICO} = \left(\int_C dV\right)\sigma_{co}\frac{L_n + r}{2L_b}\Delta\phi \tag{17}$$

v) External work (W_O)

When the CFT column deforms by $\Delta\phi$, the external work done by the horizontal load (H) and the axial load (N) is given by Eq.(18).

$$W_O = \{H(L_c - L_b)\cos\phi + N(L_c - L_b)\sin\phi + NL_n\cos\phi\}\Delta\phi \tag{18}$$

By equating the sum of the internal works (W_{IC}, W_{IL}, W_{IT}, W_{ICO}) to the external work (W_O) on the basis of the virtual work law, the equilibrium equation of CFT column under the horizontal force (H) and the axial force (N) is obtained as shown in Eq.(19).

$$\begin{aligned} H(L_c - L_b)\cos\phi + N(L_c - L_b)\sin\phi + NL_n\cos\phi \\ = (\sigma_u)\left(\int \Phi_c dV\right) \\ + \left(\int_{CQ} dL + \int_{CR} dL + 2\int_{CP} dL\right)m\frac{1}{\sin\psi}\frac{L_n + r}{2L_b} \\ + \left(\int_T dV\right)(\sigma_u)\frac{r - L_n}{L_y}\frac{1}{\cos\gamma_t} \\ + \left(\int_C dV\right)\sigma_{co}\frac{L_n + r}{2L_b} \end{aligned} \tag{19}$$

According to Eq.(19), the horizontal force H under the axial force N is decided. By the use of the obtained horizontal force (H), the fixed end moment (M) of CFT column is expressed by Eq.(20).

$$M = H\{(L_c - L_b)\cos\phi + L_b - L_n\sin\phi\} + N(L_c - L_b)\sin\phi \tag{20}$$

3.3 Stress strain relation of filled concrete

The stress of filled concrete (σ_{co}) in Eq.17 is effected by the confinement of steel tube. The stress strain relation of filled concrete which is subjected to the confinement of steel tube is derived from the stub column test of CFT member.

According to the stress analysis of steel tube based on the yield function of von Mises, the axial stress of steel tube can be approximated by $\sigma_u/\sqrt{3}$. From this result the filled concrete axial stress (σ_{co}) of CFT stub column can be expressed by subtracting the steel tube axial stress from the compression load of CFT stub column (P) and shown in Eq.(21).

$$\sigma_{co}=(P-A_s\sigma_u/\sqrt{3})/A_c \tag{21}$$

in which A_s: the sectional area of steel tube, A_c: the sectional area of filled concrete.
Applying Eq.(21) to the test result of CFT stub column, σ_{co}/σ_{ce}-ε_{co} relations are obtained and shown in Fig.8. In the figure ε_{co}: compression strain of filled concrete, σ_{ce}: compression strength of confined concrete shown by Eq.(22) which was proposed by one of the authors.

$$\sigma_{ce}=\sigma_c(0.76/\rho+0.76) \qquad (22)$$

in which ρ (=$\sigma_c A_c/\sigma_u A_s$, σ_c: compression strength of concrete) is the strength ratio of filled concrete to steel tube.

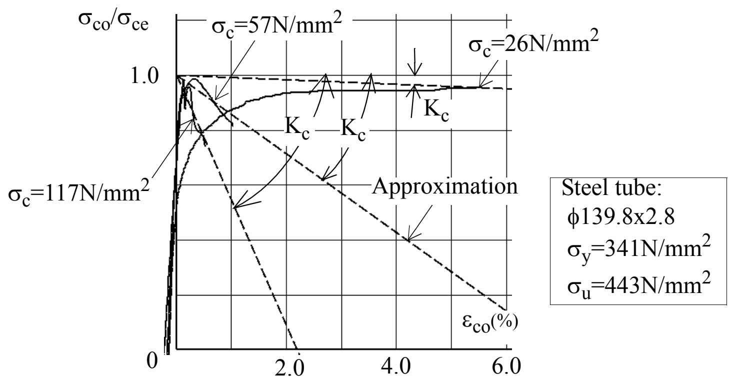

Fig.8 Compression stress-plastic strain relation of confined concrete and its model

Although the CFT column specimens are designed under the quite different conditions, the maximum compression stress of filled concrete is well predicted by the proposed confined concrete strength (σ_{ce}). We can also see all σ_{co}/σ_{ce}-ε_{co} relations are approximated by straight lines as shown in Fig.8 with the dashed lines. By expressing the gradients of σ_{co}/σ_{ce}-ε_{co} relations in the degrading state by K_c, the relation between the gradients (K_c) and the strength ratio (ρ) is obtained as shown in Fig.9. From the straight distribution of the test results of ρ-K_c relation, K_c is approximated by Eq.(23).

$$K_c= 20.7\rho \qquad (23)$$

By the use of Eq.(23), the equation to express the compression strength of filled concrete is given by Eq.(24).

$$\sigma_{co}=\sigma_{ce}(1.0-K_c\varepsilon_{co}) \qquad (24)$$

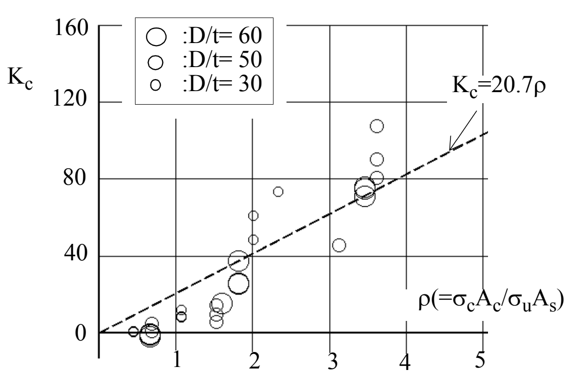

Fig.9 Gradient of stress-strain relation of confined concrete

3.4 Load-deformation relation and local buckling

The load-deformation relation of locally buckled CFT column, which is subjected to the constant axial force (N) and the horizontal force (H) at the free end, calculated by Eq.(19) and Eq.(20) is shown in Fig.10. By the calculation of the variable diameter to thickness ratio (D/t) of steel tube and the variable axial force ratio (N/Nu), the effect of them on the load-deformation relation is investigated. The material properties (σ_c, σ_u) and the aspect ratio of CFT column ($2L_c/D$) of the calculated CFT column are explained in the figure.

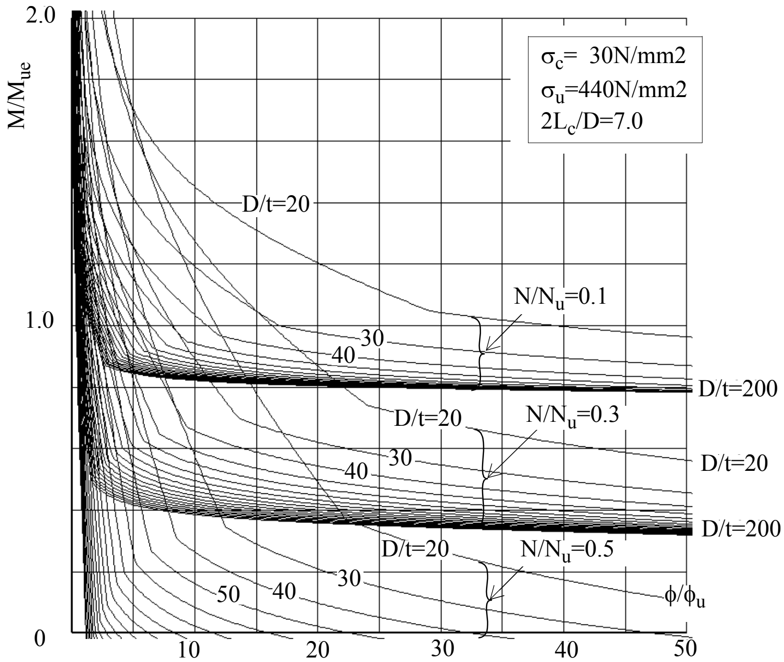

Fig.10 Load-deformation relation of locally buckled CFT column

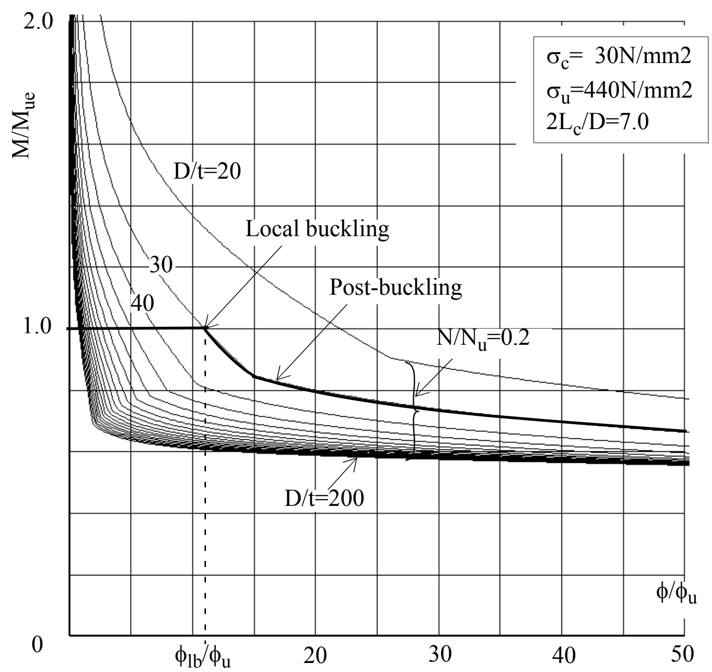

Fig.11 Load-deformation relation of locally buckled CFT column and local buckling point of steel tube

All load-deformation relations in Fig.10 show only the post-buckling behaviors and the relation before local buckling of steel tube is not calculated. The load-deformation relation of CFT column before local buckling of steel tube is given by the equation $M=M_{ue}$ as shown in Fig.11. From this reason the load-deformation relation of CFT column is expressed by the thick line in Fig.11 and the CFT column deformation (ϕ_{lb}) when the steel tube buckles locally is decided by the intersection of the two load-deformation relations as explained in Fig.11.

4. PLASTIC DEFORMATION CAPACITY ON THE BASIS OF LOCAL BUCKLING

4.1 CFT column deformation (ϕ_{lb})

The plastic deformations of CFT column (ϕ_{lb}) when the steel tube buckles locally are calculated systematically by the proposed method mentioned above and the results are shown in Fig.12(A)-Fig12(C). In the figures N/N_u and $2L_c/D$ are the axial force ratio and the aspect ratio of CFT column respectively. The chain lines in the figures show the criteria of the diameter to thickness ratio in the Japanese design code of CFT structure.

It is clearly shown that the plastic deformation capacity defined by ϕ_{lb}/ϕ_u ($\phi_u=M_{ue}/K_o$, K_o: elastic bending stiffness) changes with the well known diameter to thickness ratio of steel tube (D/t). But not only by D/t, the value of ϕ_{lb}/ϕ_u is extremely effected by the axial force ratio (N/N_u), the aspect ratio ($2L_c/D$) and the material properties (σ_c, σ_u) of CFT column. Fig.12(A)-Fig.12(C) also show that the ductile CFT columns with excellent plastic deformation capacity are in the criteria of the diameter to thickness ratio shown by the chain lines.

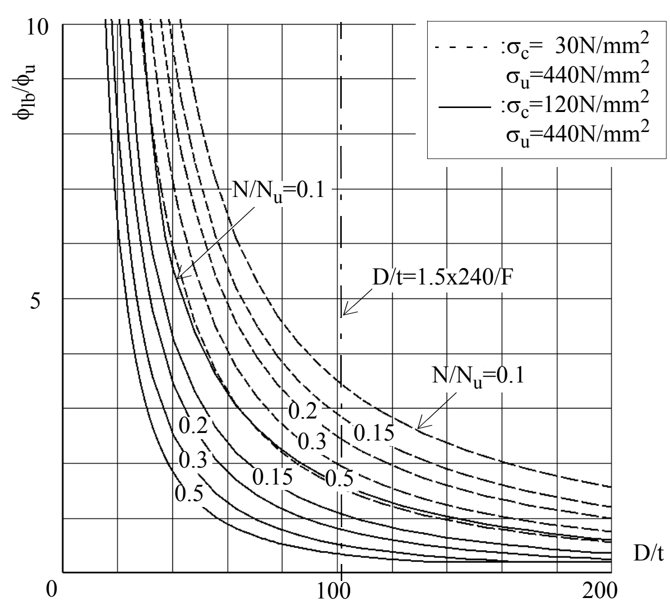

Fig.12(A) Plastic deformation until CFT-column buckles locally (Aspect ratio $2L_c/D$=4.0)

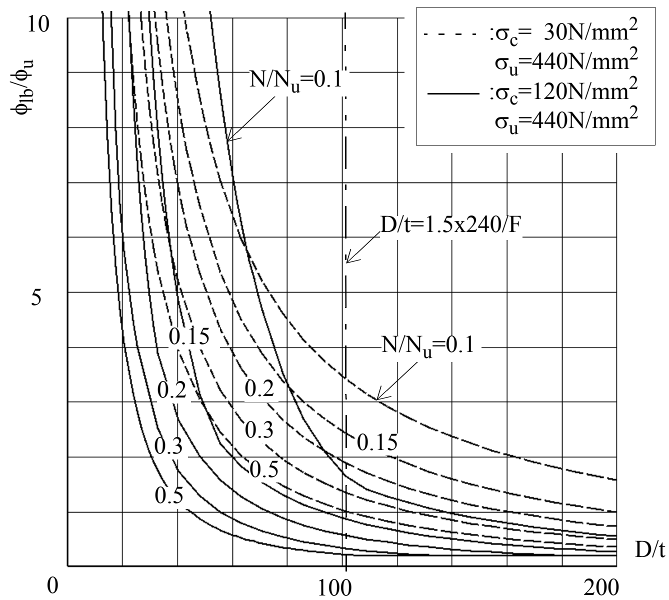

Fig.12(B) Plastic deformation until CFT-column buckles locally (Aspect ratio $2L_c/D$=7.0)

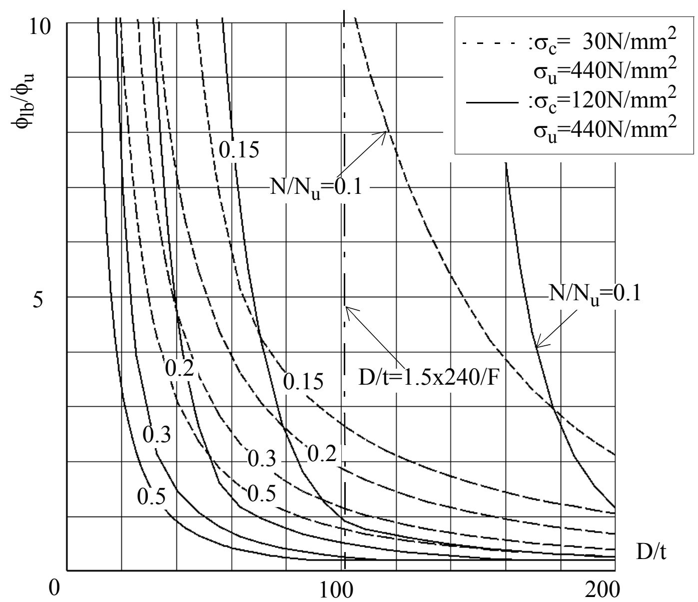

Fig.12(C) Plastic deformation until CFT-column buckles locally (Aspect ratio $2L_c/D$=10.0)

4.2 Plastic deformation capacity of experiment

The plastic deformation capacity calculated by the proposed method $(\phi_{lb}/\phi_u)_A$ is compared with test result $(\phi_{lb}/\phi_u)_T$ which is obtained by the use of steel tube strain as mentioned in the section 1.2. They are shown in Table.2(A)-2(C) and Fig.13. In the figure the plastic deformation capacities under monotonic load and repeated load are expressed.

The plastic deformation capacity under repeated load is decided by the plastic deformation between the

deformation reverse point (R) and the strain reverse point (B) as explained in Fig.14. Strictly speaking, the strain reverse point (B) in Fig.14 shows the deformation after the local buckling and it does not give the plastic deformation when steel tube buckles locally. From this reason the test results are larger than the calculated plastic deformation capacity by the proposed method. But we can say the test results under monotonic load and repeated load are approximated by the calculated plastic deformations of CFT column.
From these results it is also ascertained that CFT column ductility defined by local buckling of steel tube is effected not only by the well known D/t but also effected by the axial force ratio (N/N_u), the aspect ratio ($2L_c/D$) and the material properties (σ_c, σ_u) of CFT column.

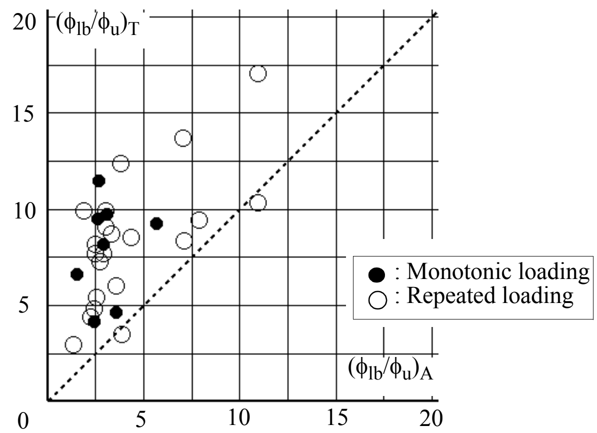

Fig.13 Plastic deformations of analysis result and test result until CFT-column buckles locally

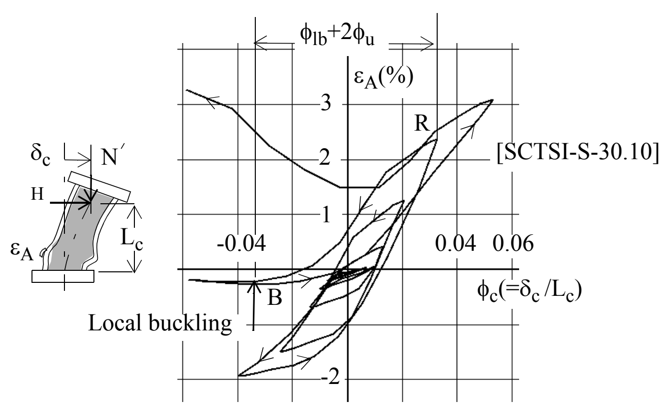

Fig.14 Relation between axial strain of steel tube and column deformation to express the local buckling point

5. CONCLUSIONS

Local buckling of concrete filled steel tube column (CFT column) is analyzed on the upper bound theorem of the limit analysis. The collapse mechanism of the analysis is assumed on the basis of CFT column test under monotonic and repeated load. The load deformation relations of many CFT columns designed under quite different conditions are calculated by the proposed analysis method and the plastic deformations until the local buckling of steel tube are also obtained.
From the calculated results it is shown that the local buckling of CFT column is closely related not only to

the well known D/t but also to the axial force ratio (N/N_u), the aspect ratio ($2L_c/D$) and the material properties (σ_c, σ_u) of CFT column.

REFERENCES

1) Saisho,M. and Goto,K., "Restoring Force Model of Concrete Filled Steel Tube Column under Seismic Load", Proceedings of 6th Pacific Structural Steel Conference (PSSC2001), Vol.1, 2001.10., pp.453-458. (Beijing, China)
2) Saisho,M. and Matsuyama,T., "Restoring Force Characteristics and Model of Concrete Filled Steel-Tube Column", Proceedings of the 12th World Conference on Earthquake Engineering (New Zealand), Paper No.1090, 2000.1.
3) Mitsunari,K. and Saisho,M., "Ultimate Strength and Plastic Deformation Capacity of CFT Beam-Column Subjected to Dynamic Load", Proceedings of the 11th World Conference on Earthquake Engineering (Mexico), Paper No.414, 1996.6.
4) Saisho,M., "Seismic Response and Collapse of Concrete Filled Steel Tube Frame under Extremely Strong Ground Motion", Proceedings of 6th Pacific Structural Steel Conference (PSSC2001), Vol.1, 2001.10., pp.441-446. (Beijing, China)
5) Saisho,M., "Dynamic Collapse of CFT-Frame under Extremely Strong Ground Motion", Proceedings of the 13th World Conference on Earthquake Engineering (Canada), Paper No.1877, 2004.8.
6) Saisho,M. and Goto,K., "Ultimate Earthquake Resistant Capacity of CFT-Frame", Proceedings of the 13th World Conference on Earthquake Engineering (Canada), Paper No.2613, 2004.8.